# Homogeneous cooling state of a system of 3D rod particles

S.M. Rubio-Largo[a], F. Alonso-Marroquin[b], T. Weinhart[c],
S. Luding[c], R.C. Hidalgo[a]

[a]*Department of Physics and Applied Mathematics, University of Navarra, 31080 Pamplona, Navarra, Spain*
[b]*School of Civil Engineering, The University of Sydney, Sydney NSW 2006, Australia*
[c]*Multi Scale Mechanics, CTW, UTwente, 7500 AE Enschede, Netherlands*

**Abstract**

In this work, we present theoretical results on granular gases of friction-less 3D rods with low dissipation. We have identified a homogeneous cooling state for rods, where the time dependence of the system intensive variables occurs only through a global granular temperature. We have found a homogeneous colling kinetics, which is in excellent agreement with Haff's law, when using an adequate rescaling time $\tau(d)$, depending on particle elongation $d$. Similarly to a system of ellipsoids, energy equipartition holds for low dissipative systems of elongated rods. Taken in advantages of scaling properties, we have numerically determined the general functionality of the magnitude $\mathcal{D}_c$, which describes the efficient of the energy interchange between rotational and translational degrees of freedom, as well as its dependence with the particle shape. Moreover, we have found there is region for the particle elongation, where the average energy transfer between the rotational and translational degrees of freedom is greater for rods than for ellipsoids, with the same aspect ratio. Although the results presented here are focused on frictional-less rods, it is important to remark that the implementation of rough rods is straightforward.

*Keywords:* Granular systems. Homogeneous cooling. Rods. Numerical Methods.

## 1. INTRODUCTION

Granular materials are daily manipulated in many industrial process and everyday life. That's why the description of their kinetic and mechanical properties is a very active research field. These systems have been deeply analyzed experimentally, analytically and numerically [1, 2], but the still produce relevant and unexpected results [1, 2].

Granular gases are very dilute systems of macroscopic grains, which move randomly loosing energy with constant rate due to their inelastic collisions. Thus, in the absence of any external driving, their energy uniformly decreases reaching a homogeneous cooling state (HCS). In that conditions, the time dependence of all its intensive variables occurs only through the global granular temperature [3, 4]. For very dissipative systems, however, the HCS becomes unstable and the system subsequently evolves into an inhomogeneous state where the cooling process notably slows down [5, 6]. Consequently, the correlation between the particle's motion determine the rate of energy lost and large inhomogeneities in the density field are observed [5, 7].

There are also experimental evidences of materials with variable restitution coefficient that depends on the relative velocity of the interacting particles. Moreover, a number of theoretical studies have carefully analyzed the particle-particle interaction during the collision, explaining how inelasticity emerges from such interactions [8, 9, 10]. For soft grains, in which the repulsion force depends linearly on deformation, a constant restitution coefficient can be recovered [11, 12] and, consequently, a cooling kinetics according to Haff law should always be expected. Contrary, assuming nonlinear elastic repulsive force (Hertzian contact) leads to a notably different algebraic decay of the system energy during the HCS [9].

On the other hand, in granular gases the particle roughness leads to correlations between the translational and rotational degrees of freedom [13, 14]. In general, both translational and rotational kinetic energies decrease with the same rate but differ from each other due to the breakdown of energy equipartition. Years ago, these correlations have been quantified for system of agitated rough spheres [15, 16]. More recently, simulations of 3D gases of rough spheres have shed light on the nontrivial process or energy interchange between the translational and rotational degrees of freedom, showing that the spin of a single grain can be correlated with the particle linear velocity [17, 18].

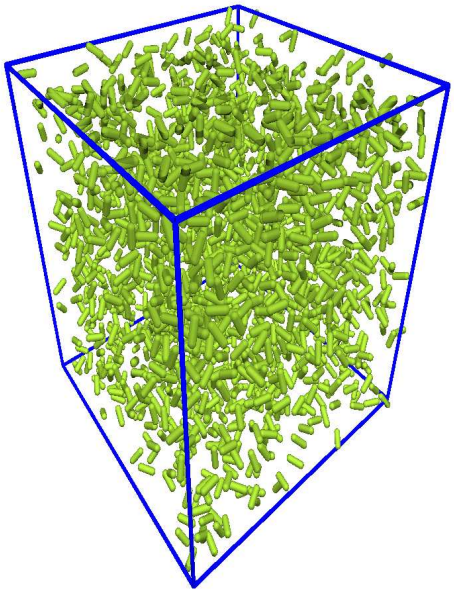

Figure 1: Snapshot of 32768 3D spheropolygons with a volume fraction $\nu = 0.04$.

Finally, much less is known about the kinetic evolution of system composed by anisotropic particles [19, 20]. However, recently there has been an increasing interest in the behavior of non-spherical grains both experimentally [21, 22, 23, 24, 25, 26] and numerically [27, 28, 29, 30]. In the present work, we investigate the free cooling process of a granular gas of elongated 3D particles. In the next sections, we analyze the role of the inelasticity and the particle shape in the overall kinetic processes.

The paper is organized as follows: in Sec. 2 we introduce some basic concepts about the kinetic of granular gases, in Sec. 2 we described the numerical model and implementation of our algorithm, Sec. 4 discusses the results of the homogeneous cooling state of a system of friction-less rods and finally we present our conclusions and outlook.

## 2. Homogeneous colling state of rods

In a gas of spherical particles of radio $a$ in HCS, the kinetic energy decreases homogeneously and the time evolution of all variables occur only through its global temperature. By introducing the dimensionless translational $T = T_{tr}(t)/T_{tr}(0)$ and rotational temperatures $R = T_{rot}(t)/T_{tr}(0)$ as well as a characteristic time $\tau$, Luding *et al* [31] have found that the kinetics of a granular gas of rough spheres is governed by the system of equations,

$$\begin{aligned} \frac{d}{d\tau}T &= -AT^{3/2} + BT^{1/2}R \\ \frac{d}{d\tau}R &= BT^{3/2} - CT^{1/2}R \end{aligned} \tag{1}$$

where $A$, $B$ and, $C$ are constants that depend on space dimensionality $D$ (further details in [31]).

$$\begin{aligned} A &= \frac{1-\epsilon_n^2}{4} + \eta(1-\eta) \\ B &= \frac{\eta^2}{q} \\ C &= \frac{\eta}{q}\left(1 - \frac{\eta}{q}\right) \end{aligned} \tag{2}$$

where $\eta = \frac{q(1+\epsilon_t)}{(2q+2)}$ (in 3D $q = \frac{2}{5}$ for spheres) and $e_n$ and $e_t$ are the restitution coefficients on the normal and tangential direction respectively. The equilibrium Enskog collision rate for the initial temperature $T_{tr}(0)$ reads as $G_{sph}(a) =$

$8(2a)^2\frac{N}{V}\sqrt{\frac{\pi}{m}}g(2a)T_{tr}^{1/2}(0)$. This variable is commonly used to rescale real time scale accordingly to $\tau = \frac{2}{D}G_{sph}t$, and $D$ accounts for the number of translational degree of freedom. It has been found that in general the principle of equipartition does not necessary apply, resulting asymptotically that $T_{tr}(\tau)/T_{rot}(\tau) \neq 1$.

On the other hand, the HCS of systems of friction-less ellipsoids has been recently examined [27, 30] In that case, the total intern energy $T_{tot}(t)$ of the gas is a weighted average of $T_{tr}$ and $T_{rot}$ with the weights given by the respective degrees of freedom:

$$T_{tot}(t) = \frac{3}{5}T_{tr}(t) + \frac{2}{5}T_{rot}(t). \tag{3}$$

Villemot and Talbot have found that for a gas of friction-less elongated ellipsoids equipartition holds [27] and, accordingly, the energy stored by the rotational $T_{rot}(t)$ and translational $T_{tr}(t)$ degrees of freedom equally evolve in time, finding asymptotically $T_{tr}(t)/T_{rot}(t) \approx 1$. Those results motivated us to examine the HCS of dissipative friction-less rods.

Assuming the existence of a (HCS) of friction-less rods, one could argue that the mean field scheme may also apply to a dilute gas of rods. It is also known that in case the the principle of equipartition fully applies $T_{tr}/T_{rot} = 1$, the energy lost can be totally described by the particles restitution coefficient $e_n$. In that case, the evolution of the granular temperature would obey Haff's Law[32]:

$$\frac{T_{tr}(t)}{T_{tr}(0)} = \frac{1}{(1+\alpha G_{rd}(d)t)^2} = \frac{1}{(1+\tau^2)}, \tag{4}$$

where $\alpha = \frac{1-e_n^2}{2D}$. The constant $D$ is interpreted as the number of degrees of freedom among which energy is transferred. We consider a gas compose by spherocylinders with aspect ratio $d$, with $d = (l+2r)/2r$ where $r$ and $l$ are the radio and length, respectively. For the cooling dynamics of this system, we propose a new characteristic time, $\tau = \alpha G_{rd}(d)t = \alpha\mathcal{D}_c(d)G_{sph}t$, which is written in terms of the collision frequency $G_{sph}$ of a sphere with the same volume. Additionally, $\mathcal{D}_c(d)$ measures the average energy transfer between rotational and translational degrees of freedom due to collisions. For the case of ellipsoids, there is an analytical expression of $G_{ellip}(d)$ [27], but in the case of rods the analytic description is still lacking. In this paper we took advantage of the homogeneous properties of the HCS of rods to numerically found the functionality of $\mathcal{D}_c(d)$.

## 3. Numerical Model

We have developed a hybrid GPU-CPU discrete element algorithm for simulating three-dimensional spherocylinders. The present implementation is based on a similar algorithm of rough spheres [33] that has been recently introduced in CUDA (Couputer Unified Device Architecture), which is a parallel computing platform invented by NVIDIA [34]. The application developed, as most of the GPGPU software, has an heterogeneous architecture. This means that some pieces of code run on the CPU and others on the GPU.

In the model, the rods are considered as sphero-cylinders, which are characterized by their length $l$ and spheroradius $r$. To calculate the contact interaction, $\vec{F}_{ij}$, we use a efficient algorithm proposed by Alonso-Marroquín et al [35, 36], allowing the simulation of a large number of particles. This numerical method is based on the concept of spheropolygons, *i.e* a polygon $i$ is defined by the set of vertexes $V_i$ and edges $E_i$. Hence, the interaction is equivalent to the inter-penetration between the two neighboring spheres. Thus, the force $\vec{F}_{ij}$ exerted on particle $i$ by the particle $j$ is defined by:

$$\vec{F}_{ij} = -\vec{F}_{ji} = \sum_{ij}\vec{F}(V_i, E_j) + \sum_{ji}\vec{F}(V_j, E_i) \tag{5}$$

where $F(V,E)$ represents the force between the vertex $V$ and the edge $E$ of each contacting pair $ij$. Hence, the local interaction between two contacting particles is only governed by the overlap distance $\delta$ between vertex and edges. In Eq.5, each term $F(V,E)$ can be decomposed as $\vec{F}(V,E) = F^N\cdot\hat{\vec{n}} + F^T\cdot\hat{\vec{t}}$, where $F^N$ is the component in normal direction $\vec{n}$ to the contact plane. Complementary, $F^T$ is the component acting on the tangential direction $\vec{t}$. To define the normal interaction $F^N$, we use a linear elastic force proportional to the overlap distance $\delta$. To account for dissipation, a velocity dependent viscous damping is assumed. Hence, the total normal force reads as $F^N = -k^N\delta - \gamma^N m_r v_{rel}^N$, where $k^N$ is the spring constant in the normal direction, $m_r = \frac{m_i m_j}{(m_i+m_j)} = \frac{m}{2}$ stands for the pair's reduced mass, $\gamma^N$ is the

damping coefficient in the normal direction and $v_{rel}^N$ is the normal relative velocity between $i$ and $j$. The tangential force $F^T$ also contains an elastic term and a tangential frictional term accounting for static friction between the grains. Taking into account Coulomb's friction constrain, which reads as, $F^T = \min\{-k^T\xi - \gamma^T m_r \cdot |v_{rel}^T|, \mu F^N\}$, where $\gamma^T$ is the damping coefficient in tangential direction, $v_{rel}^T$ is the tangential component of the relative contact velocity of the overlapping pair. $\xi$ represents the elastic elongation of an imaginary spring with spring constant $k^T$ at the contact [37], which increases as $\frac{d\xi(t)}{dt} = v_{rel}^T$ as long as there is an overlap between the interacting particles [37, 38]. $\mu$ is the friction coefficient of the particles. Although the implementation is already generalized for frictional particles, later on we will only refer to non-frictional cases.

The Newton's equation of motion of the rods particles $i$ ($i = 1, ..., N$) read as,

$$\sum_{j=1}^{N_c} \vec{F}_{ij} \quad = \quad m\ddot{\vec{r}}_i \tag{6}$$

for the translation degrees of freedom. Complementary, the *Euler*'s equations describe the rotational motion,

$$\begin{aligned}
\sum_{j=1}^{N_c} \tau_{ij}^x &= M_i^x = I_{xx}\,\dot{\omega}_{ij}^x - (I_{yy} - I_{zz})\,\omega_i^y\,\omega_i^z \\
\sum_{j=1}^{N_c} \tau_{ij}^y &= M_i^y = I_{yy}\,\dot{\omega}_{ij}^y - (I_{zz} - I_{xx})\,\omega_i^z\,\omega_i^x \\
\sum_{j=1}^{N_c} \tau_{ij}^z &= M_i^z = I_{zz}\,\dot{\omega}_{ij}^z - (I_{xx} - I_{yy})\,\omega_i^x\,\omega_i^y
\end{aligned} \tag{7}$$

In the expressions, $m$ represents the mass of the particle and $I_{xx}, I_{yy}, I_{zz}$ are the eigen-values of the moment of inertia tensor $I_{ij}$. $\mathbf{F}_{ij}$ is the force exerted by particle $j$ on particle $i$ and $\tau_{ij}$ accounts for its corresponding torque $\tau_{ij}$. The total force $\mathbf{F_i}$, and momentum $\mathbf{M_i}$ acting on particle $i$ are obtained as sums of the pair-wise interaction of particle $i$ with its contacting neighbors.

We have developed function integrators, for both the translation and the rotational degree of freedom. To integrate the 3D translational equations of motion a Verlet-velocity numerical algorithm have been implemented.

The numerical implementation of the rotational degree of freedom deserves a more detailed description. The set of Eqs(7) describes the evolution of the particles angular velocity $\omega$, in the body frame. Additional equations are necessary to describe the evolution of the particle orientation, We adopted here the quaternion representation, which has several demonstrated technical advantages over other methods [39]. The unit quaternion $q = (q_0, q_1, q_2, q_3) = q_0 + q_1 i + q_2 j + q_3 k$ characterizes the particle orientation ([40, 41]) where $\sum_{i=0}^{3} q_i^2 = 1$. Each quaternion variable satisfies the rotational equation of motion [40, 41]

$$\dot{q} = \frac{1}{2} Q(q)\omega \tag{8}$$

where

$$\dot{q} = \begin{pmatrix} \dot{q}_0 \\ \dot{q}_1 \\ \dot{q}_2 \\ \dot{q}_3 \end{pmatrix}, \quad Q(q) = \begin{pmatrix} q_0 & -q_1 & -q_2 & -q_3 \\ q_1 & q_0 & -q_3 & q_2 \\ q_2 & q_3 & q_0 & -q_1 \\ q_3 & -q_2 & q_1 & q_0 \end{pmatrix}, \quad \omega = \begin{pmatrix} 0 \\ \omega_x \\ \omega_y \\ \omega_z \end{pmatrix}.$$

Equations (7) and (8) are solved using a Fincham's leap-frog algorithm [42]. The approach obtains $q(t + dt)$ from $q(t)$ using

$$q(t + dt) = q(t) + dt\,\dot{q}(t) + \frac{dt^2}{2}\ddot{q}(t) + O(dt^3) = q(t) + dt\,\dot{q}\Big(t + \frac{dt}{2}\Big) + O(dt^3) \tag{9}$$

Hence, quaternion derivative at mid-step $\dot{q}(t + dt/2)$ is required. Equation (8) indicates that $q(t + dt/2)$ and $\omega(t + dt/2)$ are required, the former can be easily calculated using

$$q\Big(t + \frac{dt}{2}\Big) = q(t) + \dot{q}(t)\frac{dt}{2} \tag{10}$$

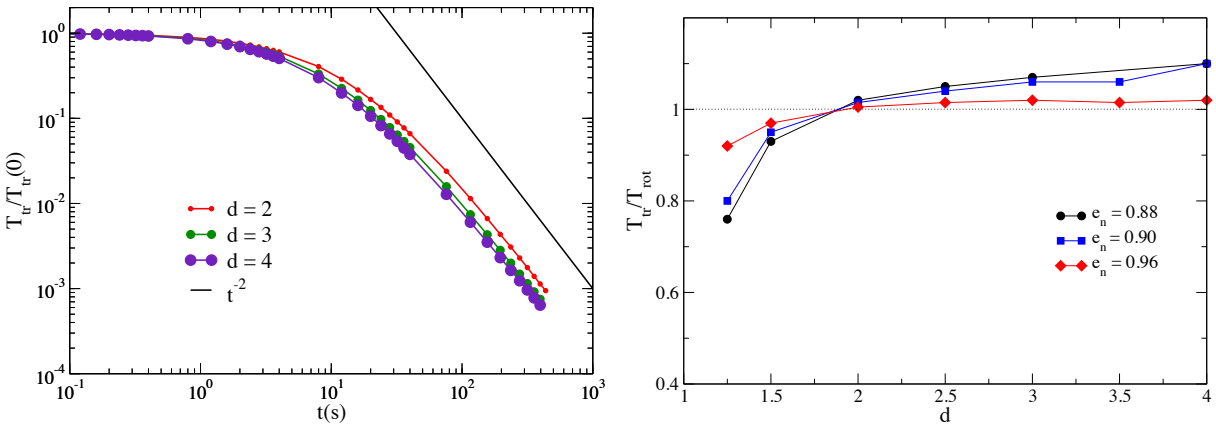


Figure 2: In a) the evolution of the kinetic energy of several systems of rods with $e_n = 0.88$; in b) the ratios between the rotational $T_{rot}(t)$ and the translational kinetic energy $T_{tr}(t)$ are also shown.

where $\dot{q}(t)$ is again obtained from (8), prior to which $\omega(t)$ can be calculated using

$$\omega_x(t) = \omega_x\Big(t - \frac{dt}{2}\Big) + \Big[\frac{I_{yy} - I_{zz}}{I_{xx}}\,\omega_y\Big(t - \frac{dt}{2}\Big)\,\omega_z\Big(t - \frac{dt}{2}\Big) + \frac{M^x}{I_{xx}}\Big]\frac{dt}{2} \tag{11}$$

$$\omega_y(t) = \omega_y\Big(t - \frac{dt}{2}\Big) + \Big[\frac{I_{zz} - I_{xx}}{I_{yy}}\,\omega_z\Big(t - \frac{dt}{2}\Big)\,\omega_x\Big(t - \frac{dt}{2}\Big) + \frac{M^y}{I_{yy}}\Big]\frac{dt}{2} \tag{12}$$

$$\omega_z(t) = \omega_z\Big(t - \frac{dt}{2}\Big) + \Big[\frac{I_{xx} - I_{yy}}{I_{zz}}\,\omega_x\Big(t - \frac{dt}{2}\Big)\,\omega_y\Big(t - \frac{dt}{2}\Big) + \frac{M^z}{I_{zz}}\Big]\frac{dt}{2} \tag{13}$$

in the same way $\omega\Big(t + \frac{dt}{2}\Big)$, is determined as,

$$\omega_x\Big(t + \frac{dt}{2}\Big) = \omega_x\Big(t - \frac{dt}{2}\Big) + \Big[\frac{I_{yy} - I_{zz}}{I_{xx}}\,\omega_y\Big(t - \frac{dt}{2}\Big)\,\omega_z\Big(t - \frac{dt}{2}\Big) + \frac{M^x}{I_{xx}}\Big]dt \tag{14}$$

$$\omega_y\Big(t + \frac{dt}{2}\Big) = \omega_y\Big(t - \frac{dt}{2}\Big) + \Big[\frac{I_{zz} - I_{xx}}{I_{yy}}\,\omega_z\Big(t - \frac{dt}{2}\Big)\,\omega_x\Big(t - \frac{dt}{2}\Big) + \frac{M^y}{I_{yy}}\Big]dt \tag{15}$$

$$\omega_z\Big(t + \frac{dt}{2}\Big) = \omega_z\Big(t - \frac{dt}{2}\Big) + \Big[\frac{I_{xx} - I_{yy}}{I_{zz}}\,\omega_x\Big(t - \frac{dt}{2}\Big)\,\omega_y\Big(t - \frac{dt}{2}\Big) + \frac{M^z}{I_{zz}}\Big]dt \tag{16}$$

To avoid build-up errors, the quaternions $q(t)$ are renormalized every time step.

The parameters of the contact model are chosen as follows: to model hard particles the maximum overlap must always be much smaller than the particle size. This have been ensured by introducing values for normal elastic constant, $k_n = 2.8 \times 10^6$. The normal dissipation parameter $\gamma_n$ is related with the normal coefficient of restitution $e_n$ by the equation $\gamma_n = \sqrt{(4k_n m_{12})/((\frac{\pi}{\ln 1/e_n})^2 + 1)}$. For frictional-less rods we have set $\gamma_t = 0$ and $k_t = 0$. The collision time can be estimated $t_c = \pi\sqrt{m_{12}/k_n}$, accordingly a time $\Delta t = t_c/50$ have been used. To compare the numerical simulations with existing analytical predictions, systems of particles with different restitution coefficients were studied, $e_n = 0.88,\ 0.90,\ 0.96$.

## 4. Simulation Results

We have numerically studied the free cooling kinetics of a dilute granular gas of rods. In all simulations reported here, a fixed number of particles ($N = 2^{15} = 32768$) confined in a square box of size $L = 2\ m$ is used. Simulations have been performed with rods of different aspect radios, from $d = 1.25$ to $d = 4$, with $d = (l + 2r)/2r$ but always keeping

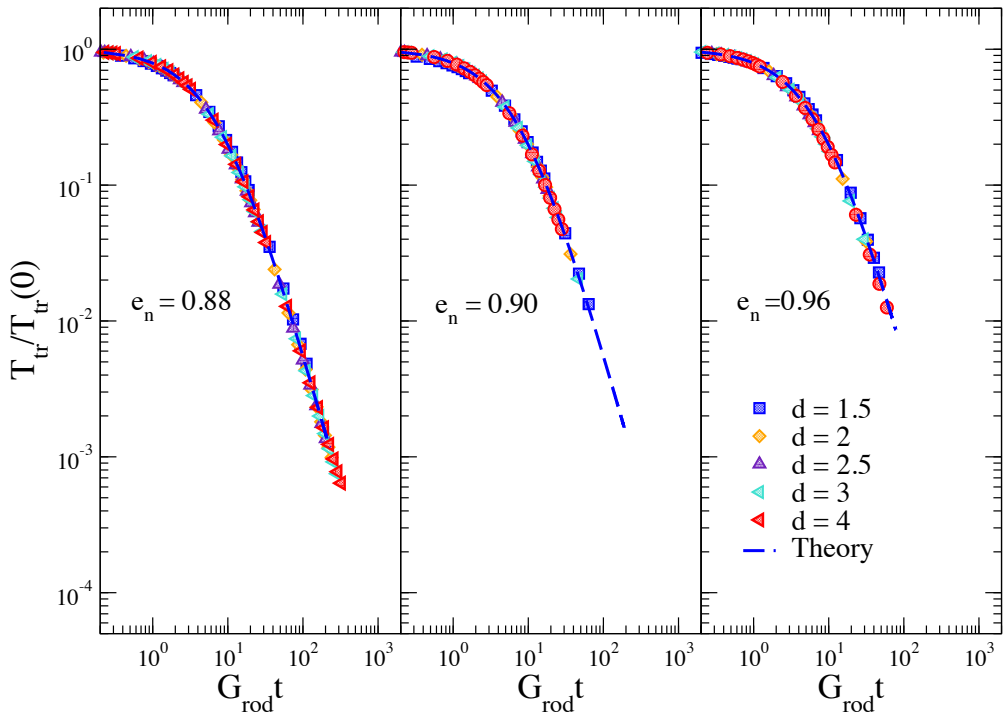


Figure 3: Collapse of the curves $T_{tr}/T_{tr}(0)$ vs $G_{rd}t = \mathcal{D}_c(d)G_{sph}t$ for each $e_n$ is illustrated. Theoretical result correspond to the numerical solution of the system of equations 1 with similar volume fraction and $e_t = 1$

the packing fraction equal to $\nu = 0.045$; in each case the values of $r$ and $l$ have been adjusted to the choice of $nu$ and $d$. Initially, the particles are homogeneously distributed in the space and their translational and rotational velocities follow a uniform distribution. To minimize finite size effects, periodic boundary conditions are implemented. Moreover, with the aim of avoiding the initial configuration effects, the dissipation is initially disabled, and a number of *free iterations* is performed. After that, the energy loss is enabled and the main loop of the program set up. The simulations are allowed to run until the total mean translational and rotational kinetic energies have decayed several orders of magnitude. In Fig.1 we display a snapshot of the simulation.

We have quantified the temporal evolution of freely evolving gases of rods by monitoring the mean translational and rotational kinetic energy of the system, usually referred as granular temperatures. In Fig. 4, the evolution of the translational kinetic energy $T_{tr}$ in time is presented. Very similar the spheres, a gas of rods cools down uniformly. Due to the low dissipation, in all cases the system seems to go into a HCS where the granular temperature asymptotically decreases following Haff's law $t^{-2}$. Complementary in Fig. 4b, the asymptotic ratio of $T_{tr}/T_{rot}$ is examined varying the elongation and the coefficient of normal restitution. Note that one observes two regions, in the case of short rods $d < 1.5$ the translational degree of freedom cools down faster than the rotational one $T_{tr}/T_{rot} < 1$. For longer rods, however, energy equipartition is better satisfied, $T_{tr}/T_{rot} = 1$, especially as one gets closer to the elastic limit $e_n = 1$. These findings indicate that the coupling between the rotational and translational degrees of freedom is more efficient as the particle gets longer. Consequently, the correlations between the linear and the angular movement are stronger and energy equipartition is achieved earlier. This behavior has also been observed in granular gases of monodisperse ellipsoids [27].

In Fig.3 the time evolution of the kinetic translational energy is compared to the mean field analytical results, which are available for a gas of spheres with similar macroscopic properties [31]. The time scale has been rescaled with its corresponding geometrical factor $G_{rd} = \alpha\mathcal{D}_c(d)G_{sp}$. Note that the only free parameter is $\mathcal{D}_c$, which has been used as fitting parameter between analytical prediction (solving Eqs. 1 with similar volume fraction and $e_t = 1$) and the numerical data obtained in our simulations. It is remarkable that all curves with different aspect ratios

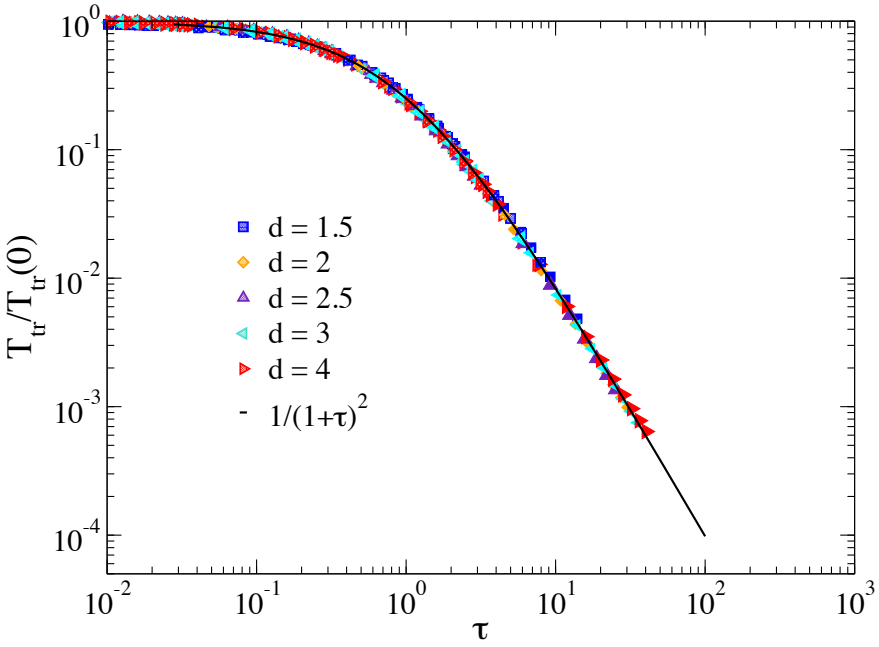


Figure 4: Scaling of all the curves when using the characteristic time $\tau = \alpha \mathcal{D}_c(d) G_{sp} t$, numerical data corresponding to several particles elongations $d > 1.5$ and restitution coefficients ($e_n = 0.88; 0.90; 0.96$) have been included.

collapse into the analytical prediction. This proves the existence of a HCS where energy equipartition practically fulfill $T_{tr}(t)/T_{rot}(t) = 1$. Thus the total energy of the system homogeneously decreases and the time evolution of all variables can be described only through its global translational temperature $T_{tr}(t)$.

Then we can go one step forward to test whether the nature of the system kinetics is independent of the dissipation parameters. In Fig. 4, we illustrate how Haff's Law applies to the homogeneous cooling state. The solid line corresponds to the theoretical approximation using Eq. (4), $\tau = \alpha G_{rd} t$ with $\alpha = \frac{1-e_n^2}{2D}$ setting $D = 5$, which corresponds with three translational and two rotational degrees of freedom, respectively [27]. The scaling of the curves and the remarkable agreement with the general analytical solution indicates the presence of a very homogeneous cooling process. Moreover, its consistency validates the performance of the numerical algorithm running on GPU architecture. It is important to remark, that the agreement is slightly lost as one approaches to the limit $d = 1$ (spheres). This case result singular due to the abrupt absence of torques and rotational degrees of freedom. Note that for friction-less spheres the rotational degrees of freedom are completely decoupled from the dynamic evolution of the gas. Moreover, the agreement with the analytical solution is also lost when the dissipation is enhanced. Here, we could argue that the numerical performance of the algorithm might be conditioned by the hardness of the used particle.

Fig. 5 shows the values of $\mathcal{D}_c$ obtained from the fitting with the Haffs law. The procedure allows us to numerically determinate the functionality of $\mathcal{D}_c$, which quantifies the the efficiency of the energy transfer between rotational and translation degrees of freedom and its size dependence for the case of rods. For comparison, we also include in Fig.5 data corresponding to the analytic outcomes obtained for friction-less monodisperse ellipsoids [27]. It is important to remark that even though using rods and ellipsoids with the same volume, still both geometrical shapes have different average surface area $\mathcal{S}c$. Consequently, one would have to compare the magnitude $\mathcal{D}_c\mathcal{S}c$. For sake of simplicity, the analytic values of Ref [27] have been rescaled with $\mathcal{S}c_{ellip}/\mathcal{S}c_{sph}$, the ratio of the average surface area of the excluded volume at contact for the ellipsoids $\mathcal{S}c_{ellip}$ at its corresponding sphere with the same volume $\mathcal{S}c_{sph}$. As expected, the results for rods are very close to the outcomes for ellipsoids with similar elongations. However, there is a region where the rods and ellipsoids behaves different. Hence for $(1.5 < d < 4.0)$ the average energy transfer between the rotational and translational degrees of freedom is slightly greater for rods than ellipsoids with similar elongation.

Finally, during the cooling process the velocity statistics was also examined. The simulation begins from a uniform

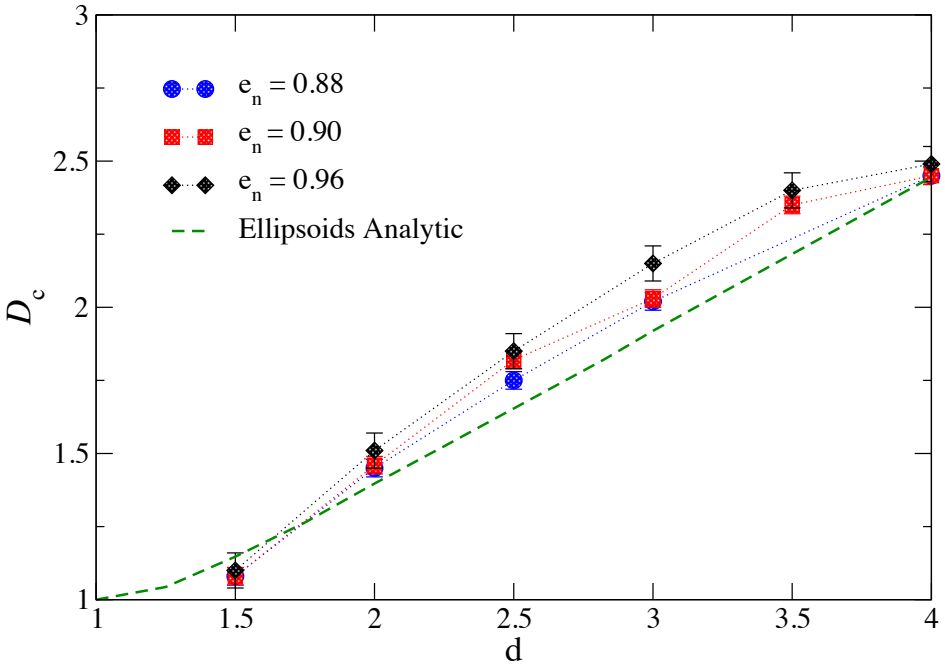


Figure 5: Numerical estimation of $\mathcal{D}_c$ as a function of the elongation, obtained collapsing each numerical data for the translational kinetic energy and its corresponding analytic prediction. For comparison, the dashed line corresponds to the theoretical result for homogeneous ellipsoids given in Ref. [27].

velocity distribution for both, the translational and angular degree of freedom. Before starting to analyze the system temporal evolution, the system is allowed to execute several hundreds of collisions without dissipation,. Note that due the low dissipation, particles cool down uniformly over a wide range of time. Thus, all the temporal dependences are calculated through the mean values of the translational and rotational temperature. The velocity distributions at different snapshot of the simuation are shown in Fig.6 a). In all cases, the velocity distributions is close to a Maxwell distribution $P(v_i) = \frac{1}{\sigma_v\sqrt{2\pi}} e^{v_i^2/2\sigma_v^2}$. For the rotational degree of freedom, in Fig.6 b) we plot the angular velocity distribution for each angular component obtained at different times. The data proves that cooling process at the rotational level also occurs homogeneously. Thus, the two components of the angular velocity behave equivalently and with the same characteristic values. In all cases the distribution follows a Gaussian behavior $P(w_i) = \frac{1}{\sigma_w\sqrt{2\pi}} e^{w_i^2/2\sigma_w^2}$ featuring the expected homogeneous cooling process. Nevertheless, finite size limitations prevents us from analyzing the tails of the distributions, where deviations from the Gaussian behavior may appear.

## Conclusions

We numerically describe a homogeneous cooling state of a granular gas of 3D spherocylindrical particles. In that state, the evolution of the system intensive variables occurs only through a global granular temperature. We examined the uniform colling kinetics and introduced rescaling time $\tau(d)$, which depends on the particle elongation. Excellent agreement with Haff's law and energy equipartition are observed for elongated particle $d > 1.5$. The agreement is enhanced when approaching to the elastic limit. Taken in advantages of scaling properties, we have numerically determined the general functionality of the magnitude $\mathcal{D}_c$, which describes the efficient of the energy interchange between rotational and translational degrees of freedom, as well as its dependence with the particle shape.

For longer times and high dissipative systems, we observe deviations from Haffs Law and clustering. Moreover, introducing particle friction has a remarkable influence on the system cooling kinetics. In that case, the azimuthal and polar rotational degrees independently evolve and only correlate with the translational degrees of freedom at very long time. These issues will be investigated in future works.

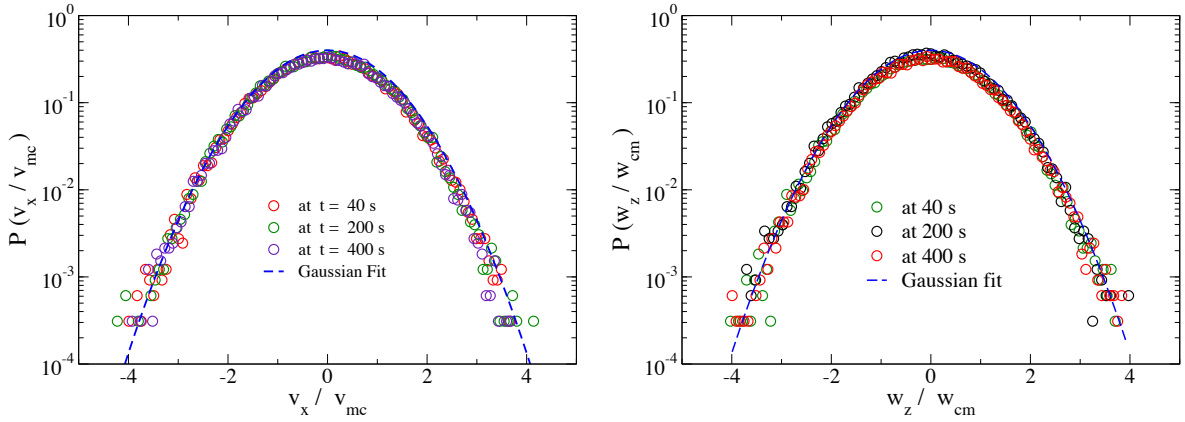


Figure 6: In a) velocity distributions and in b) angular velocity distributions obtained for a systems of friction-less rods. Results for $\epsilon_n = 0.88$ at $t = 40s, 200s, 400s$. The dashed lines correspond to a Gaussian fits.


## Acknowledgments

The Spanish MINECO (Projects FIS2011-26675), the University of Navarra (PIUNA Program) and the University of Sydney Civil Engineering Research Development Scheme (CERDS) have supported this work. S.M. Rubio-Largo thanks Asociación de Amigos de la Universidad de Navarra.


## 5. REFERENCES


[1] I. Aranson, L. Tsimring, Patterns and collective behavior in granular media: Theoretical concepts, Rev. Mod. Phys. 78 (2006) 641.
[2] T. Pöschel, T. Schwager, Computational Granular Dynamics, Springer-Verlag, Berlin , 2005.
[3] J. Brey, M. Ruiz-Montero, D. Cubero, Homogeneous cooling state of a low-density granular flow, Phys. Rev. E 54 (1996) 3664.
[4] V. Garzó, J. Dufty, Homogeneous cooling state for a granular mixture, Phys. Rev. E 60 (5) (1999) 5706–5713.
[5] S. Miller, S. Luding, Cluster growth in two- and three-dimensional granular gases, Phys. Rev. E 69 (2004) 031305.
[6] X. Nie, E. Ben-Naim, S. Chen, Dynamics of freely cooling granular gases, Phys. Rev. Lett. 89 (20) (2002) 204301, e-print cond-mat/0209412.
[7] A. Puglisi, V. Loreto, U. M. B. Marconi, A. Petri, A. Vulpiani, Clustering and non-gaussian behavior in granular matter, Phys. Rev. Lett. 81 (18) (1998) 3848–3851.
[8] T. Schwager, Coefficient of restitution for viscoelastic disks, Phys. Rev. E 75 (2007) 051305.
[9] N. Brilliantov, T. Pöschel, Velocity distribution in granular gases of viscoelastic particles, Phys. Rev. E 61 (2000) 5573.
[10] M. Shinde, D. Das, R. Rajesh, Equivalence of the freely cooling granular gas to the sticky gas, Phys. Rev. E. 79 (2009) 021303.
[11] N. Brilliantov, F. Spahn, J. Hertzsch, T. Pöschel, Model for collisions in granular gases, Phys. Rev. E 53 (5) (1996) 5382.
[12] S. Luding, Collisions & contacts between two particles, in: H. J. Herrmann, J.-P. Hovi, S. Luding (Eds.), Physics of dry granular media - NATO ASI Series E350, Kluwer Academic Publishers, Dordrecht, 1998, pp. 285–304.
[13] K. Nichol, K. E. Daniels, Equipartition of rotational and translational energy in a dense granular gas, Phys. Rev. Lett. 108 (2012) 018001.
[14] A. Sack, M. Heckel, J. E. Kollmer, F. Zimber, T. Pöschel, Energy dissipation in driven granular matter in the absence of gravity, Phys. Rev. Lett. 111 (2013) 018001.
[15] R. Cafiero, S. Luding, H. Herrmann, Two-dimensional granular gas of inelastic spheres with multiplicative driving, Phys. Rev. Lett. 84 (2000) 6014–6017.
[16] R. Cafiero, S. Luding, H. Herrmann, Rotationally driven gas of inelastic rough spheres, EPL (Europhysics Letters) 60 (2002) 854.
[17] N. V. Brilliantov, T. Pöschel, W. T. Kranz, A. Zippelius, Translations and rotations are correlated in granular gases, Phys. Rev. Lett. 98 (2007) 128001.
[18] W. Kranz, N. Brilliantov, T. Pöschel, A. Zippelius, Correlation of spin and velocity in the homogeneous cooling state of a granular gas of rough particles, The European Physical Journal Special Topics 179 (1) (2009) 91–111.
[19] T. Aspelmeier, G. Giese, A. Zippelius, Cooling dynamics of a dilute gas of inelastic rods: A many particle simulation, Phys. Rev. E 57 (1998) 857.
[20] F. Affouard, M. Kröger, S. Hess, Molecular dynamics of model liquid crystals composed of semiflexible molecules, Phys. Rev. E 54 (1996) 5178–5186.
[21] A. Kudrolli, G. Lumay, D. Volfson, L. Tsimring, Swarming and swirling in self-propelled polar granular rods, Phys. Rev. Lett. 100 (2008) 058001.
[22] T. Kanzaki, M. Acevedo, I. Zuriguel, I. Pagonabarraga, D. Maza, R. Hidalgo, Stress distribution of faceted particles in a silo after its partial discharge (2011).

[23] T. Börzsönyi, B. Szabó, G. Törös, S. Wegner, J. Török, E. Somfai, T. Bien, R. Stannarius, Orientational order and alignment of elongated particles induced by shear, Phys. Rev. Lett. 108 (2012) 228302.
[24] K. Harth, U. Kornek, T. Trittel, U. Strachauer, S. Höme, K. Will, R. Stannarius, Granular gases of rod-shaped grains in microgravity, Phys. Rev. Lett. 110 (2013) 144102.
[25] M. Acevedo, R. C. Hidalgo, I. Zuriguel D. Maza, Influence of the feeding mechanism on deposits of square particles, Phys. Rev. E 87 (2012) 012202.
[26] S. Wegner, R. Stannarius, A. Boese, G. Rose, B. Szabo, E. Somfai, T. Borzsonyi, Effects of grain shape on packing and dilatancy of sheared granular materials, Soft Matter 10 (2014) 5157–5167.
[27] F. Villemot, J. Talbot, Homogeneous cooling of hard ellipsoids, Granular Matter 14 (2) (2012) 91–97.
[28] G. Costantini, U. Marini Bettolo Marconi, G. Kalibaeva, G. Ciccotti, The inelastic hard dimer gas: a nonspherical model for granular matter., J Chem Phys 122 (16) (2005) 164505.
[29] T. Kanzaki, R. Hidalgo, D. Maza, I. Pagonabarraga, Cooling dynamics of a granular gas of elongated particles, J. Stat. Mech. 2010 (2010) P06020.
[30] D. M. S.M. Rubio-Largo, P. Lind, R. C. Hidalgo, Molecular dynamics simulation of ellipsoids: Implementation on gpu architecture, Sub. Computational Particle Mechanics.
[31] S. Luding, M. Huthmann, S. McNamara, A. Zippelius, Homogeneous cooling of rough dissipative particles: Theory and simulations, Phys. Rev. E 58 (1998) 3416–3425.
[32] P. Haff, Grain flow as a fluid-mechanical phenomenon, Journal of Fluid Mechanics 134 (1983) 401–430.
[33] R. C. Hidalgo, T. Kanzaki, F. Alonso-Marroquin, S. Luding, On the use of graphics processing units (gpus) for molecular dynamics simulation of spherical particles, AIP Conference Proceedings 1542 (1) (2013) 169–172.
[34] S. Green, Particle simulation using cuda, Tech. rep., NVIDIA Coorporation, Santa Clara, USA (May 2010).
[35] F. Alonso-Marroquín, Spheropolygons: A new method to simulate conservative and dissipative interactions between 2d complex-shaped rigid bodies, Europhys. Lett. 83 (2008) 14001.
[36] F. Alonso-Marroquín, Y. Wang, An efficient algorithm for granular dynamics simulations with complex-shaped objects, Granular Matter 11 (2009) 317–329.
[37] P. Cundall, O. Strack, A discrete numerical model for granular assemblies, Geotechnique 29 (1979) 47–65.
[38] G. Duvaut, J.-L. Lions, Les Inéquations en Mécanique et en Physique, Dunod, Paris, 1972.
[39] J. Kuipers, Quaternions and rotation sequences: a primer with applications to orbits, aerospace, and virtual reality, Princeton University Press, 2002.
[40] D. Evans, On the representation of orientation space, Molecular Physics 34 (1977) 317–325.
[41] D. Evans, S. Murad, Singularity free algorithm for molecular dynamic simulation of rigid polyatomice, Molecular Physics 34 (1977) 327–331.
[42] D. Fincham, Leapfrog rotational algorithms, Molecular Simulation 8 (3–5) (1992) 165–178.